The Maximum Standardized FDG Uptake on PET/CT in Evaluation of Patients with Non-small Cell Lung Cancer: A Prospective Study

Rania Abdalrahman Albahnasy [a*], Manal Fathey Hamisa [a],
Fatma Gharib Khirallah [b] and Hwaida M. Mokhtar [a]

[a] *Radiodiagnosis Department, Faculty of Medicine, Tanta University, Tanta, Egypt.*
[b] *Oncology Department, Faculty of Medicine, Tanta University, Tanta, Egypt.*

Authors' contributions

This work was carried out in collaboration among all authors. All authors read and approved the final manuscript.

Original Research Article

ABSTRACT

Background: Fluorodeoxyglucose Positron Emission Tomography/Computed Tomography (FDG-PET/CT) functional imaging has shown to be an invaluable non-invasive, diagnostic method, enhancing the accuracy in the presenting of Non-Small Cell Lung Cancer (NSCLC). The purpose of this research was to evaluate the role of the maximum standardized uptake value (SUV max) in PET-CT in staging and follow-up of operable and non-operable patients with NSCLC.
Methods: This prospective research carried on 50 cases with histopathological diagnosis of NSCLC were mentioned to do PET/CT scanning for initial staging of the disease (17 patients died, 28 survived, and five were lost to follow-up so 28 patients out of 50 came for follow-up after treatment with surgery, radiotherapy, or chemotherapy). All cases underwent intravenous contrast media, 18F-FDG Dosage Administration, CT Technique, PET Technique, PET-CT Fusion, and PET/CT Interpretation.
Results: SUV max is a semi-quantitative technique of determining 18F-FDG uptake by tumor cells. Adenocarcinomas have lower 18F-FDG uptake and lower SUV max measurements compared to the squamous cell carcinoma. The average SUVs of tumours ≥ 4 were significant increased compared to those < 4, and additional analysis showed that SUV max was significantly correlated with tumor size. SUV max is a prognostic factor of T and N stages as T1 lesions had a decrease

_____

*Corresponding author;

average SUV max compared to T2 and a lower mean SUV max than T3/T4 lesions, also we found that the mean SUV max of N0 is lower compared to that of NI, NII, and lower than NIII. There was a strong association among ΔSUV and Δ size.

Conclusion: FDG-PET/CT was a valuable, efficient, and reliable method of analysis in the initial staging and follow-up of lung cancer cases, and lately became a portion of the international standards in the diagnosis and the follow-up of cases with bronchogenic carcinoma.

ABBREVIATIONS

FDG : *Fluoro Deoxy Glucose*
PET/CT : *Positron Emission Tomography/Computed Tomography*
NSCLC : *Non-Small Cell Lung Cancer*
SUV max : *Maximum Standardized Uptake Value*
GLUT : *Glucose Transporters*
RT : *Radiation Therapy*
CH : *Chemotherapy*
CRT : *Concurrent Chemo-Radiotherapy*

1. INTRODUCTION

Lung cancer is the 2nd most prevalent kind of cancer in males and females.; by far the most common reason for cancer mortality cause about 25% of all cancer deaths. Histologically, it is categorized into two major types: non-small cell lung cancer (NSCLC) and small cell lung cancer (SCLC).

NSCLC was approximately 85% of lung cancer and includes the histological subtypes adenocarcinoma, large cell undifferentiated carcinoma, squamous cell carcinoma, and mixed histologies, the remaining 10-15% of cases are SCLC [1].

Adenocarcinoma is the most prevalent NSCLC subtype and represents over 40% of malignant tumours; It originates from alveolar cells in the epithelium of tiny airways. Squamous cell carcinomas were 25% to 30% of lung cancers; They often originate from cells in the airway epithelium. Large cell cancers were about 5% to 10% all lung tumours, and the prevalence is decreasing owing to modern immunophenotyping methods, enabling a more accurate categorization of badly discriminated squamous cell and adenocarcinomas. Typically, these tumours are comprised of big cells with an abundance of cytoplasm and huge nucleoli [1-3].

The evaluation of cases with expected lung tumor has usually involved morphology image estimation, using X-rays of the chest or Computed Tomography (CT) chest. More recently, the emergence of combined Positron Emission Tomography/Computed Tomography (PET/CT) imaging has significantly assisted the study of lung cancer by enabling even more precise identification of regions with elevated tracer uptake. This modality has assisted radiologists in avoiding the technical challenges connected to the independent combining of PET and CT exams, which resulted in significant artefacts; Consequently, PET/CT is now used as a diagnostic technique, as well as for disease staging and post-therapy assessment in lung cancer cases [4,5].

Fluorodeoxyglucose PET-CT determines the standardized uptake value (SUV) of a lung tissue, which assesses the tumour's glucose avidity. Fluorodeoxyglucose PET-CT has showed to be efficient for assessing staging mediastinal lymph nodes, an unspecified pulmonary nodule, and evaluating local nodal and distant metastases, also associated with tumour proliferative activity and is an independent predictive factor in cases of lung cancer [6]. The purpose of this research was to evaluate the role of the SUV max in PET-CT in staging and follow-up of operable and non-operable patients with NSCLC.

2. PATIENTS AND METHODS

This prospective research was performed in the period from June 2021 to May 2022, a total of 50 cases had histopathological diagnosis of NSCLC were involved in this research, their ages ranged from 22 to72 years. They were assigned to the department of diagnostic radiology and medical imaging at Tanta University to perform PET/CT scanning for initial staging of the disease (17 cases died, 28 survived, and five were lost to follow-up so 28 patients out of 50 came for follow-up after treatment with either surgery, radiotherapy, or chemotherapy). The inclusion criteria were patients who were proven histopathologically to have NSCLC regardless of their sex. The exclusion criteria were cases with

histopathology other than NSCLC, contraindication to the procedure (severe diabetes, severe illness, active infection, and renal disease). Uncontrolled hyperglycemia. If the patient is unable or not willing to remain still for a prolonged period. Patients have recent chemotherapy or radiotherapy (within three weeks).

PET/CT was done for all patients using a current hybrid PET/CT system [Philips Medical System (Cleveland), Germinin TF (Time-of-Flight) 16 MDCT scanner, USA], consisting of a donated PET scanner combined with a 16 multi detector CT scanner. Both CT and PET abilities in two sequential gantries, avoiding the demand for cases motion between CT and PET components. This devoted system permitted the purchase of co-recorded CT and PET images.

Imaging Technique: All cases were requested to fast for 6 hours prior to the scan. All our cases were urged to avoid consuming beverages containing caffeine or alcohol and asked to void prior to scanning. were advised to avoid a diet strong in carbohydrates and permitted a high protein diet and liquids, good control of blood glucose is important.

Serum glucose regularly calculated before 18F-FDG injection. Diabetic cases ought not to have routine insulin taken subcutaneously in 4 hours from FDG administration.

Pre-procedural evaluation of the cases' height, weight, and serum creatinine were made. The ante-cubital intravenous cannula and 18F-FDG injection were administered. Prior to the procedure, patients were urged to remain calm in the injection room for 60 minutes and to refrain from any intense activity, including chewing.

The contrast media used: Intravenous contrast media was used in 46 patients out of 50 patients with NSCLC participated in this study, while it was contraindicated in 4 patients as they had renal impairment and their serum creatinine levels (> 2 mg/dl).

18F-FDG Dosage Administration: An average of 5–10 mCi (0.14 mCu/kg) of 18FDG was administered for each patient. The cases waited 45 to 60 minutes following receiving FDG., This period, known as the absorption phase, is necessary for the biodistribution of FDG properly and delivered into the cells of the case, cases were instructed to consume as much water as possible to flush away any residual radioactive particles, stay in a quiet place, and they preserve their motility.

The cases were presented with the PET-CT device, sitting supine with the head immobilized and the arms raised for image enhancement.

A PET scan of the entire body (neck to pelvis) is followed by an improved CT scan of the entire body. Approximately, The CT scan takes 60–70 seconds, while the PET scan takes 20–30 minutes.

CT Technique: Single-phase contrast material–enhanced helical CT is done after injection of 125 mL of a low-osmolarity iodinated contrast medium (ioversol; Optiray 350) at a range of 4 mL/sec by a power injector. Overall CT coverage size equals the number of scanned bed positions through the gathering of PET information. At 2.4 mm intervals, the helical data are retrospectively rebuilt.

PET Technique: The PET scanner is situated within the same lengthy gantry as the CT scanner and is placed behind it. After the CT scan, PET is done without moving the patient. In the three-dimensional acquisition mode, approximately six to seven bed postures are scheduled for imaging the complete case, with an acquisition time of five to seven minutes each bed position. 145 centimetres is the longest length which may be examined using the existing PET-CT scanner.

PET-CT Fusion: After PET acquisition is complete, PET images reconstructed with attenuation correction, CT, and fused images of corresponding PET and CT scans are accessible for evaluation using the manufacturer's review station in axial, coronal, and sagittal planes and in maximum-intensity projections, 3-dimensional cine mode.

PET/CT Interpretation: The CT, PET, and fused PET-CT images were assessed regarding the primary tumor and existence of lymph nodes and distant metastases. Using the SUV max, a semiquantitative analysis was conducted, and the lesion of the highest SUV max was determined for every group. SUV = mean region of interest activity (MBq/g)/injected dose (MBq)/body weight was the default method used to calculate SUV (g). Each case's main tumours were arranged based on the TN eighth edition category. Between pre- and post-treatment

follow-up 18F-FDG-PET/CT scans, a average gap of 4 months (range: 3–5 months) was observed.

Based on the recommendations of the European Organization for Research and Treatment of Cancer (EORTC) characteristics for PET, the time point of the metabolic reaction was determined [7]. Complete metabolic response (CMR) was attained after the SUVs of all lesions dropped to the same point as the surrounding tissues. PMR was percent alteration of the sum of SUVs ($\triangle$SUV%) < −25%; stable metabolic disease (SMD) was −25% ≤ $\triangle$SUV% < 25%; and progressive metabolic disease (PMD) was $\triangle$SUV% ≥ 25%, when the degree of 18F-FDG improved greater than 20% in the greatest distance, or when new 18F-FDG uptake occurred in metastatic lesions. The gold standard for CT interpretation was the RECIST criteria. On CT images, NSCLC was evaluated based on its size. According to RECIST criteria1, patients having a complete response (CR) or partial response (PR) were later categorized as responders [8]. Those that experienced stable disease (SD) or progressing disease were considered nonresponses. $\triangle$SUV% and $\triangle$lesion size% determined by the subsequent formulas: $\triangle$SUV= [(post-treatment SUV max-Pre-treatment SUV max)/Pre-treatment SUV max] × 100 %, Δ lesion size = [(post-treatment lesion size-Pre-treatment lesion)/pretreatment size] x100%.

2.1 Case No. 1

74-year-old female case had recent histological diagnosis of right lung large cell carcinoma for staging. PET CT findings: Incomplete ring of abnormal increased metabolic activity consistent with the margin of a right upper lobe irregular thick-walled cavitary pulmonary lesion maximum thickness 2.1 cm with SUV max 11.2 (dimensions of the cavitary lesion 5.7x5.11x5.3 cm), (Liver SUV max. 2.5). Incomplete ring of abnormal increased metabolic activity is seen at the left ala of the sacrum, SUV max 12.4 (dimensions of the lesion are 5.8 x4x5cm). No pathologic FDG activity or abnormally enlarged lymph nodes.

OPINION: Known case of bronchogenic large cell carcinoma before therapy revealed: Metabolic active right upper lobe thick-walled cavitary lung lesion with osseous metastases as described. PET/CT stage T3N0M1b, Stage IVa.
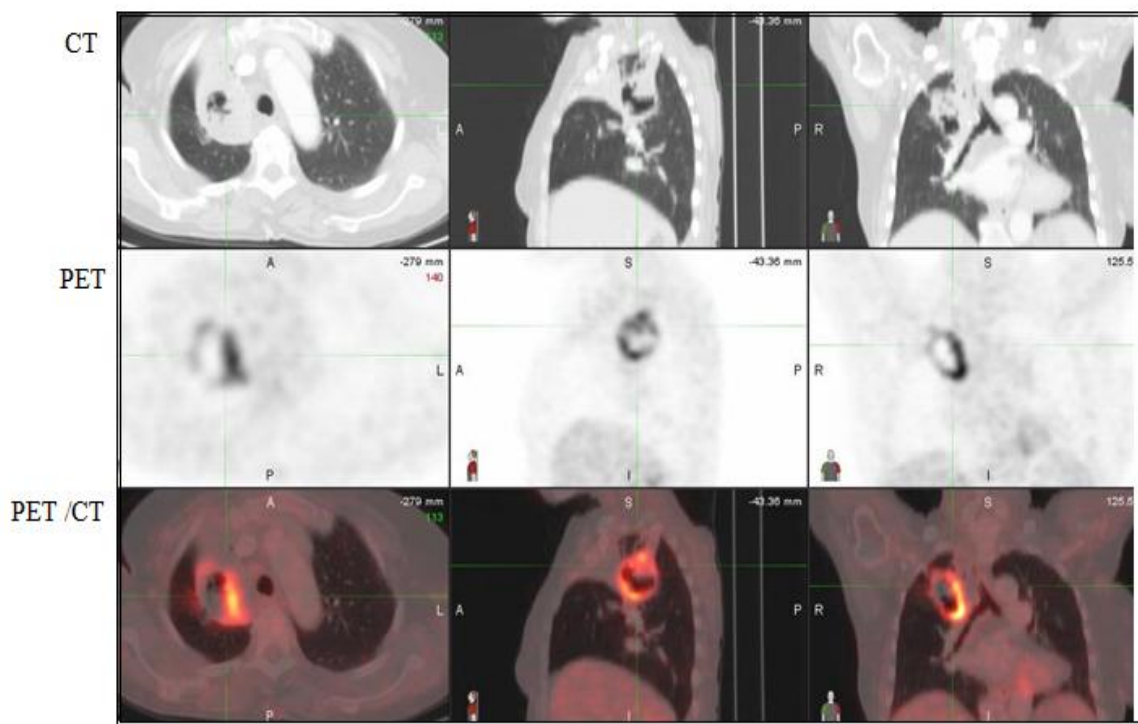

Image 1. Axial, sagittal, and coronal CT, PET, and PET/CT images showing metabolic active right upper lobe thick-walled cavitary lung lesion
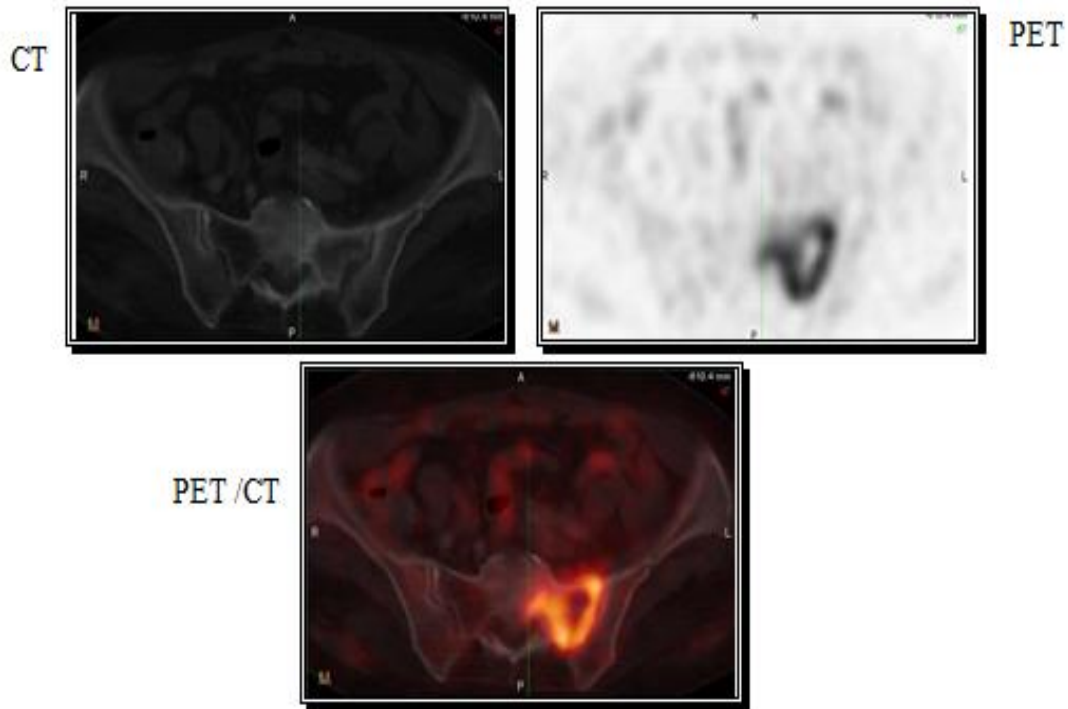
Image 2. Axial CT, PET and PET/CT image shows the left ala of the sacrum metastatic deposit

2.2 Case No. 2

A female patient aged 24 years presented with left lung Neoplastic growth (moderately distinguished adenocarcinoma), proven by biopsy during therapy, and assigned for follow-up four months later. Reason for study: For primary staging and post-chemotherapy assessment.

Primary PET/CT findings: Metabolically active pleural-based soft tissue lesion is found at the lateral segment of the left lower lung lobe with surrounding consolidation measured 4.7 x 3.5 cm with SUV max 17.5, (Liver SUV max. 2.3). Metabolic active left hilar lymph node measured 1.5 x 1.5 cm with SUV max 11.2 associated. Metabolic active Subcarinal lymph node measured 1x1 cm, SUV max 7.8. No distant metastases. Primary PET/CT staging T2bN2M0(IIIA).

Post therapy PET/CT: Metabolic and morphologic regression of the left lower lung lobe hypermetabolic neoplastic mass (presently reaching 6.6 SUV max and calculating 2.5 x2 cm (compared to 17.5 SUV max and 4.7x3.5 cm previously). Metabolically active left hilar lymph

node is seen measuring 1.5x1.5 with SUV max 4.7 (compared to SUV max 11.2 of the previous study). Near-totalal resolution of the previously described subcarinal lymph nodes. Post chemotherapy staging: T1c N1 M0 (IIB).

Impression: Regressive course of the disease in the form of decreased dimension and metabolic process of the left peripheral lung mass, decreased metabolic activity of the left hilar lymph node and total resolution of the subcarinal lymph node.

2.3 Statistical Analysis

Statistical analysis was done by SPSS v26 (IBM Inc., Chicago, IL, USA). Numerical variables were represented as mean and standard deviation (SD). Categorical variables were presented as frequency and percent (%). Standard student "t test": test of significance of the difference between two means. Analysis of variance [ANOVA] tests (f): According to the computer program SPSS for Windows. ANOVA test was used for comparison among more than two means in quantitative data.
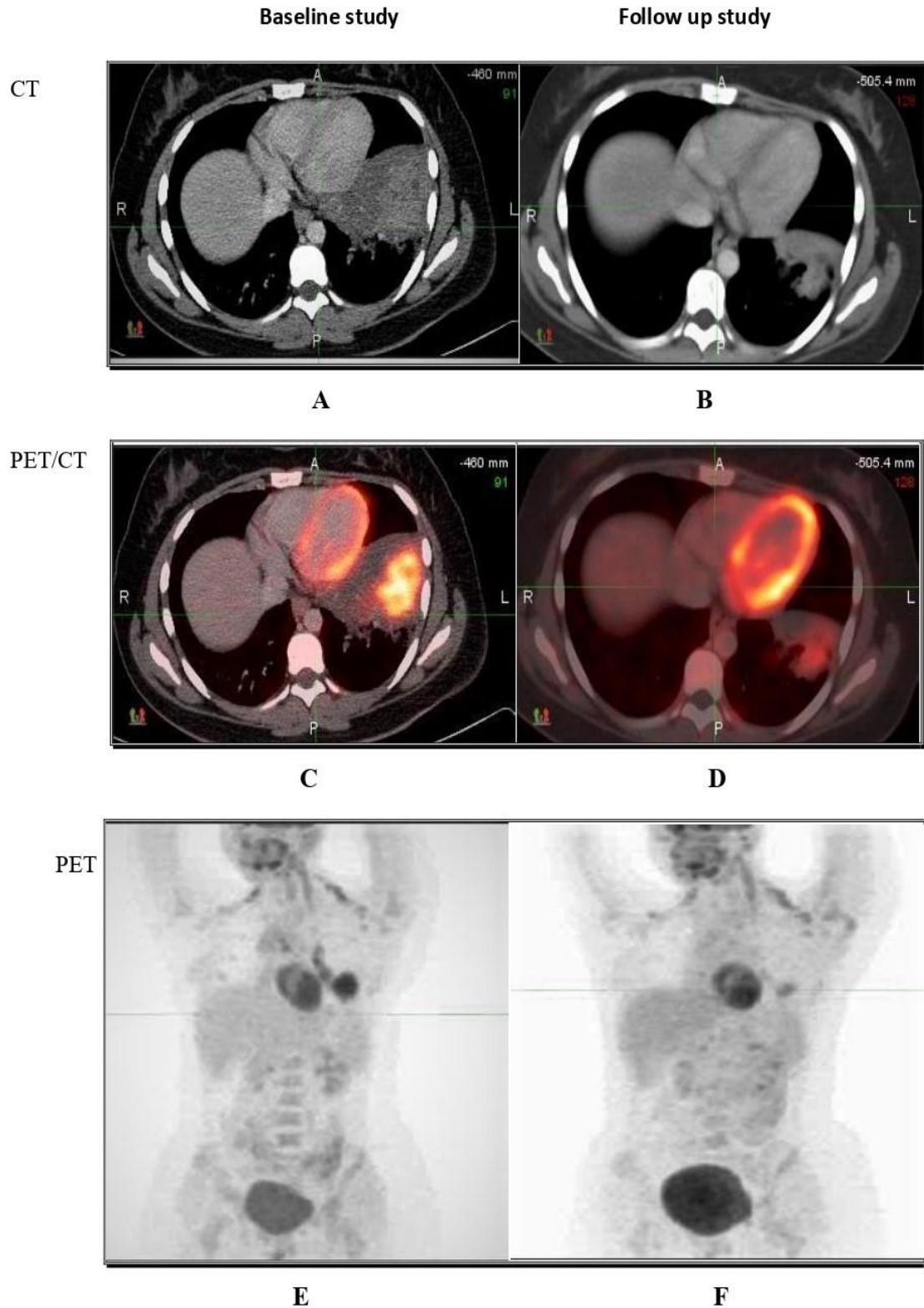
Baseline study   **Follow up study**

Image 3. (A-D). Axial CT and fused PET/CT images before and after therapy showing metabolic and morphological regression of the left lower lung lobe hypermetabolic neoplastic mass. (E, F): Whole-body MIP images before and after therapy showing marked metabolic therapeutic response

3. RESULTS

Table 1. Demographic data of the studied patients with NSCLC (n = 50)

		N	%
Age	Range	23 – 69	
	Mean ± SD	56.56 ± 9.72	
	Median	57.5	
Sex	Male	36	72
	Female	14	28
Smoking	No	18	36
	Yes	32	64
Weight	Range	50 – 125	
	Mean ± SD	85.32 ± 17.43	
	Median	86	
Height	Range	155 – 180	
	Mean ± SD	167.42 ± 6.16	
	Median	168	
Blood glucose	Range	75 – 104	
	Mean ± SD	104.22 ± 21.47	
	Median	100	

Table 2. Clinical presentation and Lobar distribution of the primary lung lesions of the studied patients

Clinical data	N	%
Cough &dyspnea	40	80
Chest pain	12	32
Hemoptysis	15	30
Paraneoplastic Syndromes	5	10
Pancoast syndrome	1	2
Other (generalized fatigue, epigastric pain, headache)	5	10
Distribution		
RLL	15	30
RML	12	24
RUL	5	10
LLL	10	20
LUL	4	5
Both lungs	4	8
Total	**50**	**100**

RLL = right lower lung lobe, RUL = right upper lung lobe, ML = Middle lobe, LLL = left lower lung lobe, LUL = left upper lung lobe

Table 3. Distribution of the studied patients according to histopathology, degree of differentiation and metastatic lesions by PET CT in the studied patients

Histopathology	N	%
Squamous cell carcinoma	25	50
Adenocarcinoma	19	38
Other (large cell carcinoma or undifferentiated carcinoma)	6	12
Total	50	100
Degree of differentiation		
Well	8	16
Moderate	16	32
Poor	26	52
Total	50	100
Site of metastatic lesion		
Bony lesions	15	30
Hepatic lesions	8	16
Brain lesions	10	20
Adrenal lesions	16	32

Table 4. The staging of patients with the 8th edition TNM system (n=50)

Stage grouping	No of patients	Percentage
IA	1	2
IB	1	2
IIA	0	0
IIB	1	2
IIIA	5	10
IIIB	4	8
IIIC	3	6
IVA	22	44
IVB	13	26
Total	50	100

Regarding correlation between SUV max and histopathology, it showed that squamous cell carcinoma had a higher mean SUV max than other histopathological kinds, also regarding Correlation among SUV max and degree of variation, results were statistically significant, also according to primary tumor size it showed that SUV max in tumours ≥ 4 was higher than that of tumours < 4 Table 5.

SUV max was significant correlated with tumor size. They raised in a tumor size-dependent manner Fig. 1.

The SUV max of the primary lung lesions was significant increased than that of the metastatic lesions Table 6.

Type of treatment for patients came for follow-up Fig. 2.

The responder post-treatment SUV and Δ SUV were decreased compared to the non-responder value. Whereas insignificant difference among the pre-treatment SUV of two groups Table 7.

Table 5. Correlation between SUV max and histopathology, tumor differentiation and primary lesion size

| SUV max	Histopathology		
	Squamous	**Adenocarcinoma**	**Other**
Range	6.4 – 18.7	5.1 – 12.5	3.1 – 10.5
Mean ± SD	12.86 ± 2.95	9.14 ± 2.52	6.88 ± 3.27
f. test	15.667		
P. value	0.001*		
	Tumor differentiation		
	Well (n=8)	**Moderate (n=16)**	**Poor (n=26)**
Mean ± SD	5.8 ± 2.6		
f. test	4.524		
P. value	0.017*		
	Primary lesion size		
	< 4	≥ 4	
Range	3.1 – 9.9		
Mean ± SD	5.89 ± 1.93		
T. test	5.782		
P. value	0.001*		
	T stages		
	T 1	T 2	T 3-4
Range	3.1 – 10.6	4.5 – 13	7.1 – 18.7
Mean ± SD	6.13 ± 2.65	8.90 ± 3.32	12.38 ± 2.61
f. test	16.161		
P. value	0.001*		
	N stage		
	N 0	N I – II	N III
Range	3.1 – 14	8.5 – 15.2	7.3 – 18.7
Mean ± SD	8.51 ± 3.29	11.41 ± 1.89	13.16 ± 3.05
f. test	12.193		
P. value	0.001*		
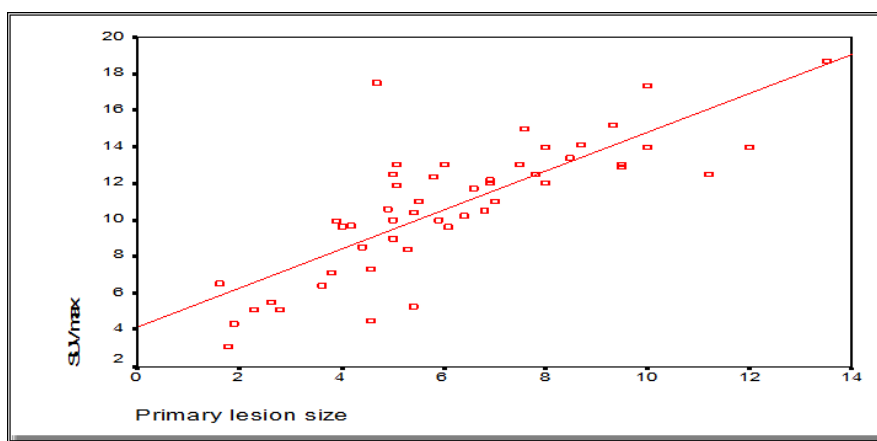
Fig. 1. Showing correlation between SUV max and primary tumor size (n=50)

Table 6. Comparison between SUV max of the primary lung lesions and metastatic lesions

Site of the lesion	SUV primary	SUV metastatic	T	P
Bone	8.4 ± 3.1	6.2 ± 2.6	2.108	0.044*
Adrenal	9.4 ± 4.2	5.5 ± 3.9	2.706	0.011*
Pleural	9.1 ± 4.9	5.1 ± 3.2	2.903	0.007*
Mediastinal lymph node	9.1 ± 4.8	6.3 ± 4.2	2.482	0.016*
Liver	9.7 ± 3.2	6.0 ± 2.7	2.501	0.025*
Intrapulmonary	9.3 ± 4.3	3.3 ± 2.1	3.958	0.001*

Table 7. Comparison between pre-treatment SUV, post-treatment SUV, and % change in SUV (ΔSUV) of the responder and non-responder groups (n=28)

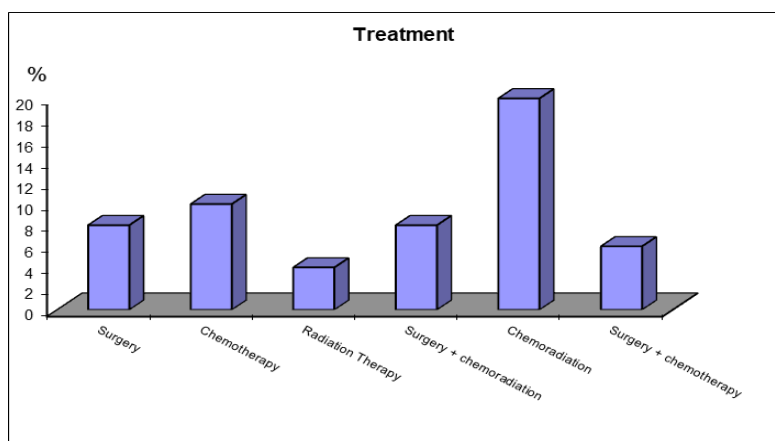|		Responder	Non-responder	P-value
Pre-TREATMENT SUV	Range	5.3 – 18.7	3.1 – 14	0.084
	Mean ± SD	12.31 ± 3.41	8.97 ± 3.52	
	Median	12	9.6	
Post -TERATMENT SUV	Range	0 – 9.4	4 – 17.5	0.001*
	Mean ± SD	5.72 ± 3.15	12.26 ± 4.63	
	Median	6.5	13.5	
Δ SUV	Range	-100 – -32.86	-21.57 – 129.69	0.001*
	Mean ± SD	-53.38 ± 23.98	40.14 ± 34.58	
	Median	-45.38	34.62	

Fig. 2. An image histogram showing distribution of the studied cases (n=28) according to treatment

Table 8. Metabolic response by PET/CT after treatment of the 28 patients

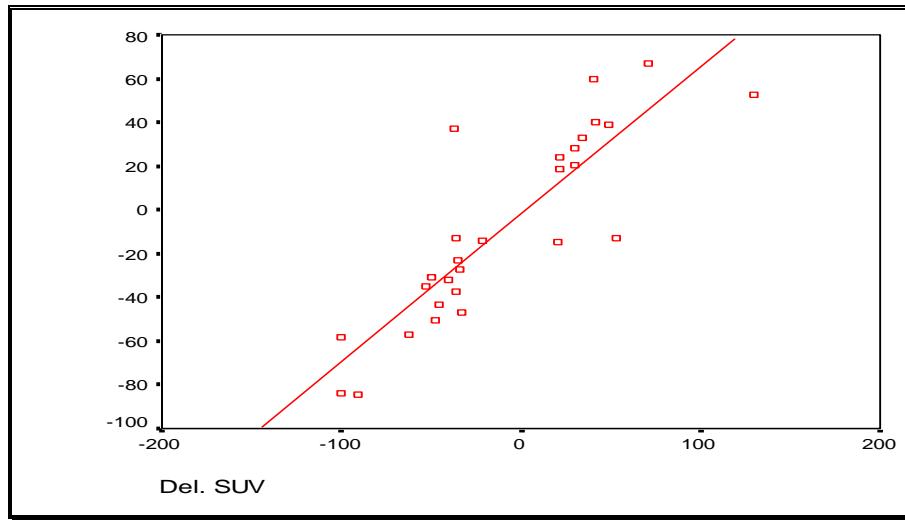| Metabolic response	N	%
Complete	3	10.7
Partial	12	42.9
Stable	4	14.3
Progressive	9	32.1
Total	28	100

Fig. 3. Scatter diagram displaying the strong positive correlation between ΔSUV and ΔSIZE in all patients

The strongest correlation was shown between ΔSUV and Δ size shown in Fig. 3.

4. DISCUSSION

NSCLC is regarded as a rapidly growing disease. Surgery, radiation therapy, chemotherapy, and genotype-driven medicines are among the treatment methods [9]. Currently, concurrent chemoradiation therapy (CRT) is the preferred neoadjuvant therapy for patients with operable illness [10].

Recently, 18F-Fluorodeoxyglucose Positron Emission Tomography/Computed Tomography (18F-FDG PET/CT) has become a powerful tool in the management of lung cancer due to its ability to assess regional lymph node spread more precisely than CT scan and to detect metastatic lesions that would be missed or ambiguous with conventional imaging [11].

Our agreed with the study done by Duan, et al. [12] studied 74 patients and found that 54 patients were males while 14 were females, however, Kohutek, et al. [13] found that 92 patients were men, and 119 cases were women

and cases ranged in age from 23 to 69, with a average age of 56.56± 9.72 years.

In agreement with Sheikhbahaei et al. [14] who stated that a history of smoking was existing in 156 cases (77.6%).

In agreement with Ganie et al. [15] who stated that cough occurs in between 70 and 90 % of patients.

As detected by Mavi et al. [16] who found that the right lung sends metastasis to the right hilar and paratracheal lymph nodes, while the left lung sends metastasis to the left hilar and paratracheal lymph nodes. Lower-lobe cancers also can send metastases to paraesophageal, and subdiaphragmatic lymph nodes [17].

Our results agreed with Al-Sarraf et al. [18] who found squamous cell carcinoma the most popular kind and in contrast with Evangelistaa et al. [19] who found adenocarcinoma the most common type.

Our outcomes were like to those of Qiu et al. [20] who noticed that the most common sites for

distant metastases at presentation were bone, adrenal, and liver.

Our findings were similar to what had been previously reported by many investigators as few signs and symptoms are present at an early stage of NSCLC, leading to more advanced disease when patients present to their physicians. Reade and Ganti et al. [21] showed that close to 75% of patients with NSCLC were presenting with illness that is localised or metastatic disease at the time of diagnosis.

In agreement with Mattoli, et al. [22] who stated that adenocarcinoma subtype had an average SUV max that was less compared to that of squamous cell subtype. This may because Adenocarcinomas express less Glut-1 transporters, resulting in reduced 18FDG absorption and SUVmax values compared to squamous cell types. In contrast to Budak et al. [23] who stated that no statistically significant difference was identified between adenocarcinoma (16.8±13.5) and SCC (17.9±5.6) in regard to mean SUV max (p=0.2).

In our research there was a relation among tumour SUV max and degree of differentiation as tumour SUV max was higher in poorly differentiated NSCLSC, that agreed with Ishibashi et al. [24].

That agreed with Duan et al. [12] who found that The average size of the initial tumour was 3.05 cm, and the average SUVs of tumours larger than 3 cm were significantly greater compared to those smaller than 3 cm (P 0.0001) and in contrast Shaheen et al. [25] with who stated that insignificant association among SUV max and primary tumor size values (P = 0.16).

In agreement with Al-Sarraf, et al. [18] who stated that T1 lesions exhibited a decrease average SUV max compared to T2 lesions and T3/T4 lesions (p =0.0001).The progression of T phases and the observed increase in SUV max could be partially illustrated by tumour volume and size. The most curable stage (stage I) had the lowest average SUV max of all phases.

In our research we found The SUV max of the primary lesions was substantially greater compared to that of the metastatic lesions (p 0.05), allowing the SUV max of the primary lung lesions to indicate the seriousness of the tumour more accurately. That agreed with Qiu, et al. [20].

In agreement with Huang et al. [26] who stated that variations in SUV max were significant decreased in responders compared to in non-responders based on RECIST criteria (84) that served as the standard.

Our results agreed with Fattah et al., Cappabianca et al. [27-29] who stated that the tumor dimension and the entity of necrosis are factors that impact the SUV max of a tumor with a positive correlation among tumor diameter and SUV max.

5. CONCLUSIONS

FDG-PET/CT established itself as a valuable, efficient, and reliable method of analysis in the primary staging and follow-up of lung cancer cases, and lately became a portion of the international standard in the diagnosis and the follow-up of cases with NSCLC.

6. LIMITATIONS

PET-CT is comparatively more costly than other techniques modalities, and This must be assessed considering the present economic context., the small sample size and it does not consider the spatial distribution of metabolic activity, as it calculates 18-FDG uptake from a single hot pixel in the tumor mass.

CONSENT AND ETHICAL APPROVAL

The research was performed after approval from the Ethical Committee Tanta University. Informed written consent was obtained from the patients.

COMPETING INTERESTS

Authors have declared that no competing interests exist.

REFERENCES

1. Takeuchi S, Khiewvan B, Fox PS, Swisher SG, Rohren EM, Bassett RL, et al. Impact of initial PET/CT staging in terms of clinical stage, management plan, and prognosis in 592 patients with non-small-cell lung cancer. European Journal of Nuclear Medicine and Molecular Imaging. 2014; 41:906-14.
2. Takamochi K, Ohmiya H, Itoh M, Mogushi K, Saito T, Hara K, et al. Novel biomarkers that assist in accurate discrimination of squamous cell carcinoma from adenocarcinoma of the lung. BMC cancer. 2016;16:1-10.

3. Travis WD, Brambilla E, Nicholson AG, Yatabe Y, Austin JH, Beasley MB, et al. The 2015 World Health Organization classification of lung tumors: impact of genetic, clinical and radiologic advances since the 2004 classification. Journal of thoracic oncology. 2015;10:1243-60.

4. Ambrosini V, Nicolini S, Caroli P, Nanni C, Massaro A, Marzola MC, et al. PET/CT imaging in different types of lung cancer: an overview. Eur J Radiol. 2012;81:988-1001.

5. Sharma P, Singh H, Basu S, Kumar R. Positron emission tomography-computed tomography in the management of lung cancer: An update. South Asian J Cancer. 2013;2:171-8.

6. de Groot PM, Chung JH, Ackman JB, Berry MF, Carter BW, Colletti PM, et al. ACR Appropriateness Criteria(®) Noninvasive Clinical Staging of Primary Lung Cancer. J Am Coll. Radiol. 2019; 16:S184-s95.

7. Young H, Baum R, Cremerius U, Herholz K, Hoekstra O, Lammertsma AA, et al. Measurement of clinical and subclinical tumour response using [18F]-fluorodeoxyglucose and positron emission tomography: review and 1999 EORTC recommendations. European Organization for Research and Treatment of Cancer (EORTC) PET Study Group. Eur J Cancer. 1999;35:1773-82.

8. Rastogi A, Baheti AD, Patra A, Tirumani SH. Tumor response criteria in oncoimaging: RECIST criteria and beyond—Part 1. Journal of Gastrointestinal and Abdominal Radiology. 2019;2:098-106.

9. Gridelli C, de Marinis F, Cappuzzo F, Di Maio M, Hirsch FR, Mok T, et al. Treatment of advanced non-small-cell lung cancer with epidermal growth factor receptor (EGFR) mutation or ALK gene rearrangement: results of an international expert panel meeting of the Italian Association of Thoracic Oncology. Clin Lung Cancer. 2014;15:173-81.

10. Aupérin A, Le Péchoux C, Rolland E, Curran WJ, Furuse K, Fournel P, et al. Meta-analysis of concomitant versus sequential radiochemotherapy in locally advanced non-small-cell lung cancer. J Clin Oncol. 2010;28:2181-90.

11. Postmus PE, Kerr KM, Oudkerk M, Senan S, Waller DA, Vansteenkiste J, et al. Early and locally advanced non-small-cell lung cancer (NSCLC): ESMO Clinical Practice Guidelines for diagnosis, treatment and follow-up. Ann Oncol. 2017;28:iv1-iv21.

12. Duan XY, Wang W, Li M, Li Y, Guo YM. Predictive significance of standardized uptake value parameters of FDG-PET in patients with non-small cell lung carcinoma. Braz J Med Biol. Res. 2015; 48:267-72.

13. Kohutek ZA, Wu AJ, Zhang Z, Foster A, Din SU, Yorke ED, et al. FDG-PET maximum standardized uptake value is prognostic for recurrence and survival after stereotactic body radiotherapy for non-small cell lung cancer. Lung Cancer. 2015;89:115-20.

14. Sheikhbahaei S, Mena E, Marcus C, Wray R, Taghipour M, Subramaniam RM. 18F-FDG PET/CT: Therapy Response Assessment Interpretation (Hopkins Criteria) and Survival Outcomes in Lung Cancer Patients. J Nucl Med. 2016;57:855-60.

15. Ganie FA, Wani ML, Lone H, Wani SN, Hussain SA. Carcinoma lung: Clinical presentation, diagnosis, and its surgical management. The Journal of Association of Chest Physicians. 2013;1:38.

16. Mavi A, Lakhani P, Zhuang H, Gupta NC, Alavi A. Fluorodeoxyglucose-PET in characterizing solitary pulmonary nodules, assessing pleural diseases, and the initial staging, restaging, therapy planning, and monitoring response of lung cancer. Radiologic Clinics. 2005;43:1-21.

17. Platt JF, Glazer GM, Gross BH, Quint LE, Francis IR, Orringer MB. CT evaluation of mediastinal lymph nodes in lung cancer: influence of the lobar site of the primary neoplasm. American Journal of Roentgenology. 1987;149:683-6.

18. Al-Sarraf N, Gately K, Lucey J, Aziz R, Doddakula K, Wilson L, et al. Clinical implication and prognostic significance of standardised uptake value of primary non-small cell lung cancer on positron emission tomography: analysis of 176 cases. European journal of cardio-thoracic surgery. 2008;34:892-7.

19. Evangelista L, Cuppari L, Menis J, Bonanno L, Reccia P, Frega S, et al. 18F-FDG PET/CT in non-small-cell lung cancer patients: a potential predictive biomarker of response to immunotherapy. Nuclear medicine communications. 2019;40:802-7.

20. Qiu X, Liang H, Zhong W, Zhao J, Chen M, Zhu Z, et al. Prognostic impact of

maximum standardized uptake value on 18F-FDG PET/CT imaging of the primary lung lesion on survival in advanced non-small cell lung cancer: A retrospective study. Thoracic Cancer. 2021;12:845-53.

21. Reade CA, Ganti AK. EGFR targeted therapy in non-small cell lung cancer: potential role of cetuximab. Biologics: targets & therapy. 2009;3:215.

22. Mattoli MV, Massaccesi M, Castelluccia A, Scolozzi V, Mantini G, Calcagni ML. The predictive value of 18F-FDG PET-CT for assessing the clinical outcomes in locally advanced NSCLC patients after a new induction treatment: low-dose fractionated radiotherapy with concurrent chemotherapy. Radiation Oncology. 2017;12:1-11.

23. Budak E, Çok G, Akgün A. The contribution of fluorine 18F-FDG PET/CT to lung cancer diagnosis, staging and treatment planning. Molecular imaging and radionuclide therapy. 2018;27:73.

24. Ishibashi T, Kaji M, Kato T, Ishikawa K, Kadoya M, Tamaki N. 18F-FDG uptake in primary lung cancer as a predictor of intratumoral vessel invasion. Annals of nuclear medicine. 2011;25:547-53.

25. Shaheen AA, Mohammed AM, Elshimy A, Shalaby MH. Role of PET/CT in post-therapeutic assessment of bronchogenic

carcinoma. Egyptian Journal of Radiology and Nuclear Medicine. 2021;52:1-12.

26. Huang W, Zhou T, Ma L, Sun H, Gong H, Wang J, et al. Standard uptake value and metabolic tumor volume of 18F-FDG PET/CT predict short-term outcome early in the course of chemoradiotherapy in advanced non-small cell lung cancer. European journal of nuclear medicine and molecular imaging. 2011;38:1628-35.

27. Cerfolio RJ, Bryant AS, Winokur TS, Ohja B, Bartolucci AA. Repeat FDG-PET after neoadjuvant therapy is a predictor of pathologic response in patients with non-small cell lung cancer. The Annals of thoracic surgery. 2004;78:1903-9.

28. Cappabianca S, Porto A, Petrillo M, Greco B, Reginelli A, Ronza F, et al. Preliminary study on the correlation between grading and histology of solitary pulmonary nodules and contrast enhancement and [18F] fluorodeoxyglucose standardised uptake value after evaluation by dynamic multiphase CT and PET/CT. Journal of clinical pathology. 2011;64:114-9.

29. Fattah A, Refaat MM, Shahin M. Role of PET/CT in staging and assessment the therapy response of lung cancer. Available: https://www researchgate net/publication/316254621_role_of_petct_i n_staging_and_assessment_the_therapy_ response_of_lung_cancer. 2017.